Experimental Study on the Rate Effect on the Shear Strength

Ryuta Saito,[1)] Hiroshi Fukuoka[2)] and Kyoji Sassa[3)]
1) Graduate School of Science, Kyoto University, Gokasyo, Uji, 611-0011, Japan (saito@landslide.dpri.kyoto-u.ac.jp)
2) Research Centre on Landslide, Disaster Prevention Research Institute, Kyoto University, Gokasyo, Uji, 611-0011, Japan (fukuoka@landslide.dpri.kyoto-u.ac.jp)
3) Research Centre on Landslide, Disaster Prevention Research Institute, Kyoto University, Gokasyo, Uji, 611-0011, Japan (sassa@scl.kyoto-u.ac.jp)

Abstract

This paper presents a relation between the shear strength and the shear rate in cohesive soils. Tests were carried out by means of an undrained ring shear apparatus on Silica sand, Silica sand-Illite mixture sample and Silica sand-Bentonite mixture sample. The pore water pressure was directly measured, and thus Residual friction angle were calculated. As a result, the dependence of effective residual friction angle on the shear rate was identified in illite or bentonite mixture sample. According to values of measured effective residual friction angle, shear mode seems to change with shear rate. This change in shear mode could be thought as the rate effect mechanism of shear strength in cohesive soil.

Keywords: Ring shear test, Residual strength, Shear rate, Rate effect

Introduction

The Residual shear strength in the shear zone is used for stability analysis of reactivated landslides and may be used to predict the behavior of the soil within sliding mass of landslides. From this point of view, a study of residual strength is applicable to predict the landslide movement. Ring shear apparatus allows long shear displacement, and many researchers have reported about the residual strength by means of this apparatus.

A significant influence on the shear rate, on the residual strength of cohesive soils, was presented by Skempton (1985), Tika *et al.* (1996), Tika *et al.* (1999), Suzuki *et al.* (2000) and Lemos (2003). Tika *et al.* (1996) described that, if a shear surface formed at residual strength by slow shear rate under drained condition, then subjected to a fast shear rate, three types of residual strength were observed: a positive rate effect in soils showing a fast strength higher than the slow residual strength; a neutral rate effect in soils showing a constant fast residual strength, equal to the slow strength; and a negative rate effect showing a significant drop in fast residual strength below the slow residual when sheared at rates higher than a critical value(Fig. 1).

Although the rate effect mechanism on residual strength has not been clarified yet, some ideas suggesting that residual strength of soils are affected by shearing rate existed: 1) an influence of a change in pore water pressure, and 2) a change in shear mode in the shear zone.

The generated pore water pressure was dependent on the strain rate in undrained triaxial tests (Matsui *et al.*, 1977). Therefore the pore water pressure in residual state may be dependent on shear rate. In other words, the dependence of effective normal stress on shear rate may cause the change in residual strength of soil.

On the other hand, Tika *et al.* (1996) suggested that a change in shear mode on shear zone caused the rate effect of residual strength. Their shear box was surrounded by a water bath, and they investigated the influence of the water in the bath. They compared the fast shear rate residual strength of soil with or without water in the bath, and observed residual strength at fast shear rate without water in the bath was higher than with water in the bath. Therefore they presented a process that the free water penetrated into the shear zone at fast shear rate, water content increased in shear zone, and thus an increase in an ability of the change in shear mode to flow.

Both ideas focused on the fact that effective residual friction angles, ϕ'_rr', were dependent on or independent of the shear rate. If the change in pore water pressure causes the rate effect of residual strength, effective residual friction angle is independent of shear rate. If the shear mode changes with shear rate, effective residual friction angle is also changed with shear rate.

The relation between effective residual friction angles and shear rates can be identified if the pore water

pp. 421–427

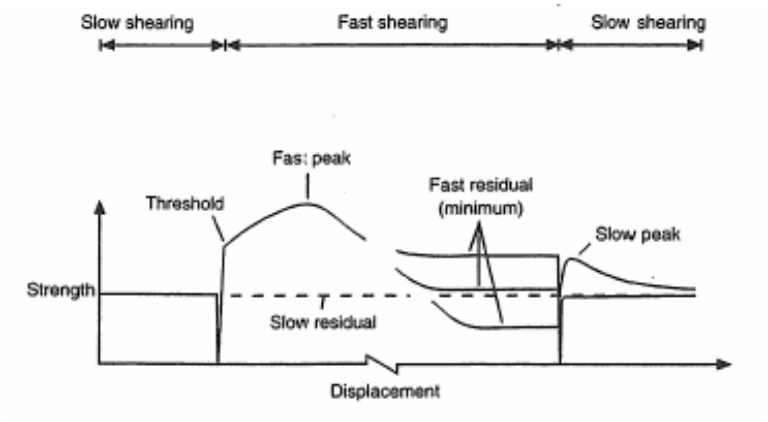

Fig. 1. Summary of the observed rate-displacement phenomena for the residual strength (after Tika *et al.*, 1996).

pressure is measured in residual state by means of a ring shear apparatus. However, in previous studies the correct measurement of pore water pressure in a ring shear test was not possible mainly due to some technical difficulties, and thus the influence of this factor is not clear at the present stage.

Thus, authors have investigated on the change of friction angle at different shear rate in use of an undrained ring shear apparatus, and presented the relation of these parameters in cohesive soil.

Apparatus and Test procedure

Ring shear apparatus

The tests were carried out by means of an undrained ring shear apparatus, DPRI-6, at Disaster Prevention Reach Institute, Kyoto University (Sassa *et al.*, 2004). The specimen was set in a doughnut-like shape in between the inner and the outer stainless shear boxes. The outer and the inner diameter are 175 mm and 125 mm respectively. The specimens were loaded normally through annular plate connected an oil piston controlled by a feed back system, and were sheared by rotating the lower shear box by servomotor, while two resistance transducers retain the upper half of shear box with measuring the shear resistance. Fig.2 shows a half section of the undrained shear box and the pore water pressure measurement of the ring shear apparatus. Rubber edges were set on lower shear boxes to prevent leakage of water and specimen during consolidation and shearing. These edges and O-rings fitted to the loading plate ensure complete undrained situation. Pore water pressure transducers were connected to a gutter cut along the whole circumference on inner wall of outer shear box located at 2 mm above the shear surface. Along the gutter, a felt cloth and two metal filters are set to separate the pore water from specimen (Sassa *et al.*, 2003).

Samples and Test procedure

The samples were industrial silica sand #8 (D_{50} = 0.04mm) called SS, Silica sand mixed with illite 10 % and 20 % by weight called I10 and I20, and mixed with bentonite 100 % and 20 % by weight called B10 and B20 respectively.

The test consisted of 8 stages with 4 different shear rates: 0.01 mm/sec, 0.1mm/sec, 1 mm/sec and 10 mm/sec (Fig.3). The specimens were saturated and consolidated at 100 kPa, and the total normal stress was kept at 100 kPa during tests. The specimens were sheared at 0.01 mm/sec (stage 1) under undrained condition. After the residual strength had been established, the shear rate was reduced to zero and the pore water pressure was disappeared under drained condition, then the specimen was re-sheared at 1 mm/sec (stage 2). This procedures, sheared and disappeared the pore water pressure, were repeated to stage 8.

Results and Discussion

Shear resistance and Pore water pressure

Figure 4 and Figure 5 show the stress-displacement diagram of sample I20 and B20 respectively. In all tests the shear resistance attained the peak strength at a practically negligible displacement, then, decreased

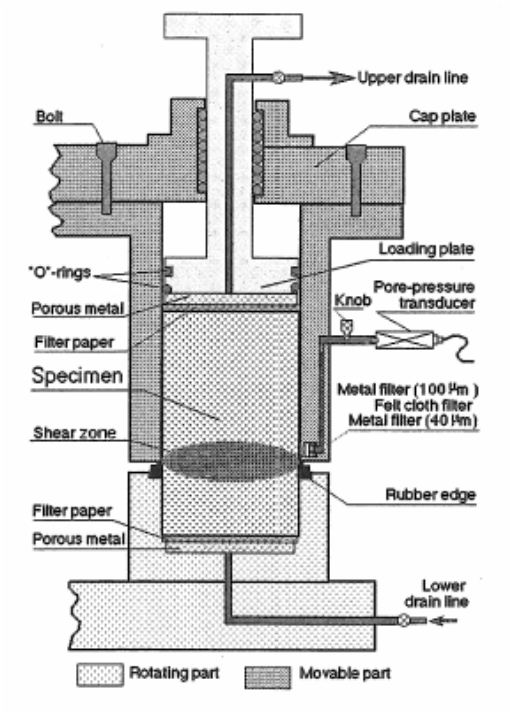

Fig. 2. A half section of the undrained shear box and the pore water pressure measurement.

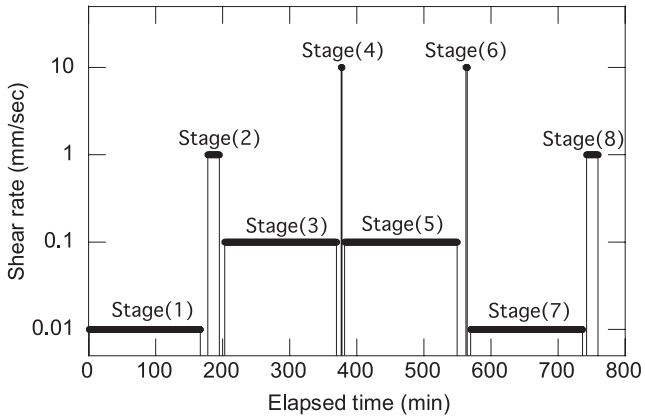

Fig. 3. Shear rate conditions in each stage of tests.

gently to the residual strength in each stage.

The typical change in the pore water pressure was observed in sample I20, as shown in figure 4. The pore water pressure tended to increase with the shear displacement.

The pore water pressure of sample B20 was measured in a different pattern from other tests. In slower shearing stages as 0.01 mm/sec and 0.1 mm/sec, the pore water pressure increased with the shear displacement. However, in faster shearing stages as 1 mm/sec and 10 mm/sec, the pore water pressure suddenly dropped to negative value.

Effective friction angle

According to measured parameters, which were total normal stress, shear resistance and pore water pressure, effective friction angle at the point was calculated by $\phi' = \tan^{-1}\{\tau/(\sigma - u)\}$. Figure 6 and Figure 7 show the friction angle-displacement diagram of sample I20 and B20 respectively.

Effective friction angel increased near the peak value at a practically negligible displacement, then performed approximately peak value, or decreased gently. Note that in sample B20 effective fiction angle decreased to significantly low values at faster shear rate stages.

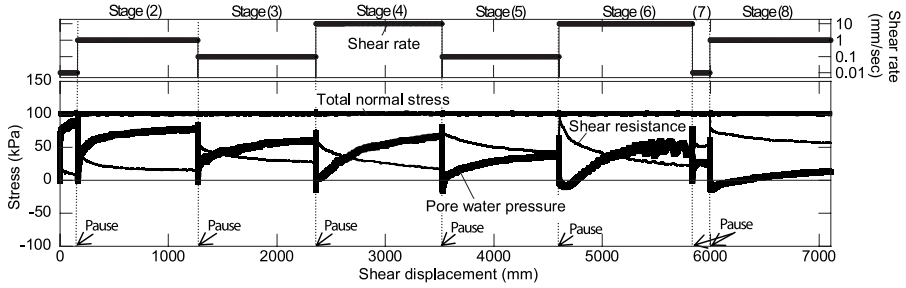

Fig. 4. Stress-displacement diagram of sample I20.

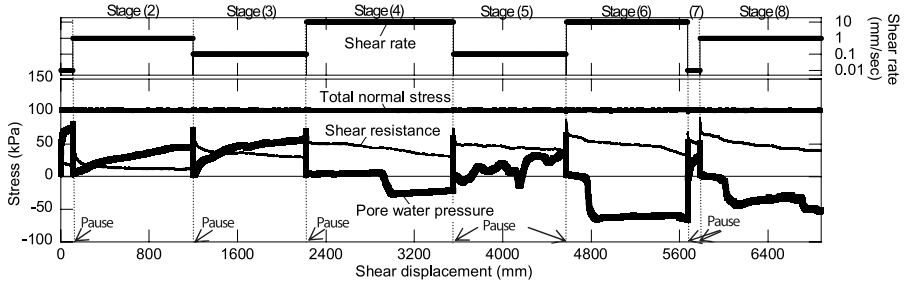

Fig. 5. Stress-displacement diagram of sample B20.

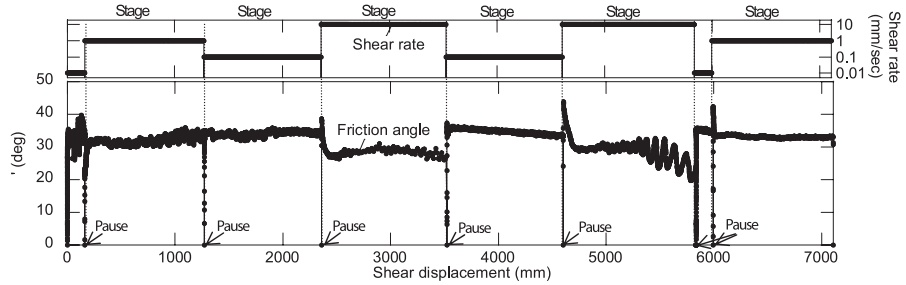

Fig. 6. Friction angle-displacement diagram of sample I20.

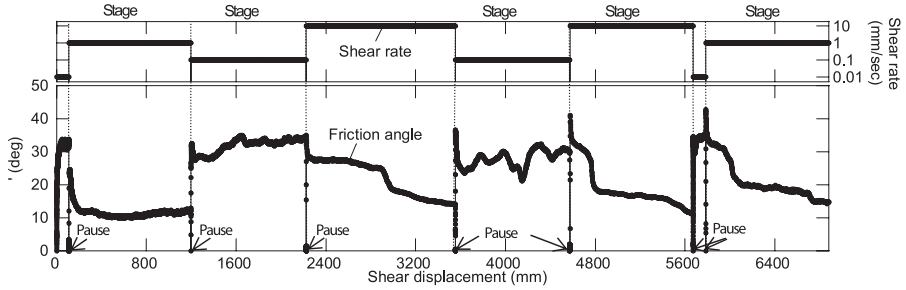

Fig. 7. Friction angle-displacement diagram of sample B20.

Failure lines-Shear rate

Figure 8 shows the stress paths in sample B20 at shear rate 0.1 mm/sec and 1 mm/sec. The stress paths reached the same failure line even if the shear rate was equal. This tendency was also observed in sample I20. This variation of failure line with shear rate, explained the difference of effective residual friction angles. Thus, indicating that the failure line of soil is dependent on shear rate.

The generated pore water pressure was independent of shear rate, so the effective normal stress was also independent. It is noted that the measured residual shear "resistance" was different between the same shear rate stages.

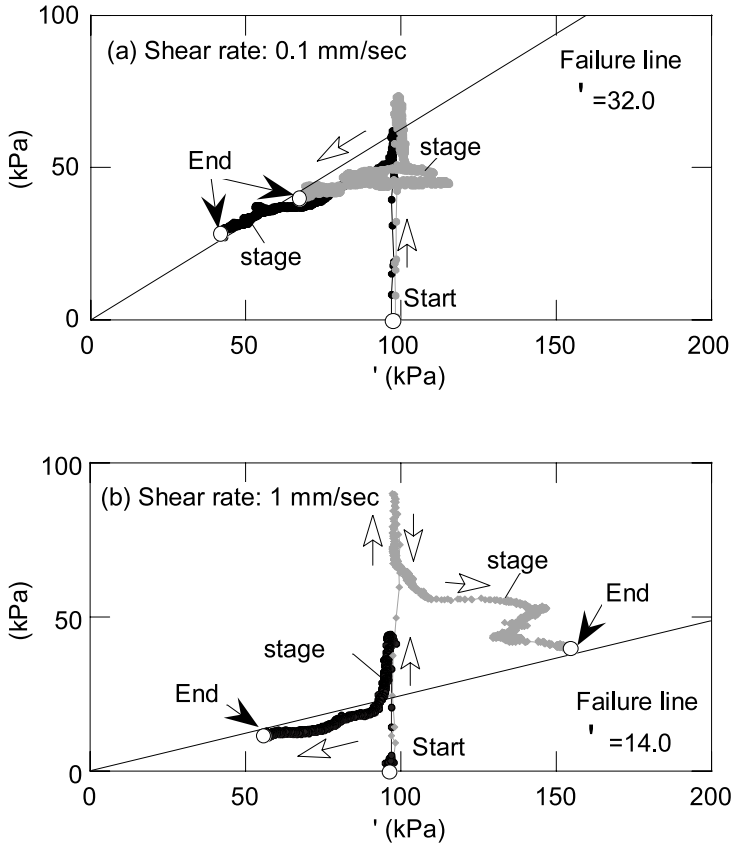

Fig. 8. Stress path of sample B20. (a) Shear rate was 0.1 mm/sec: stage 3 and 5. (b) Shear rate was 1 mm/sec: stage 2 and 8.

Effective residual friction angle-Shear rate

The relation between effective residual friction angles and shear rates are presented in Figure 9(a)–(c). Effective Residual friction angles were obtained from stress path in each stage.

Effective residual friction angles of sample SS were around 34° at all shear rate stages, and thus these angles were independent of shear rate.

In illite or bentonite mixture sample, effective residual friction angles were dependent on shear rate. Although effective residual friction angles showed constant values at all shear rate stages in sample I10, effective residual friction angles in sample I20 and B10 presented approximately equal level among at slower 1 mm/sec stages in each sample, and presented slightly lower values at 10 mm/sec than other shear rates. In sample B20 effective residual friction angles at 1 mm/sec and 10 mm/sec have presented significantly lower values than at 0.01 mm/sec and 0.1 mm/sec.

These results indicate that a sample containing illite or bentonite sample would show a negative rate effect. In addition, Figure 9 shows that the soil containing bentonite is more prone to a negative rate effect than illite.

Hypothesis for the rate effect mechanism in cohesive soil

Friction angle is thought of as a material property, reflecting the combined effect of particle friction plus the degree of interlocking (Lambe *et al.*, 1969). The difference of friction angles would be expressed as the difference of shear mode. Therefore the rate effect of effective residual friction angles can be thought of as a change of shear mode with shear rates. Sand shows friction angle approximately 35°. In sample B20 at slower shear rate stages as 0.01 mm/sec and 0.1 mm/sec, effective residual friction angles were approximately 33° as the same degree as sand friction angle (Figure 9). The shear mode in slower shear rate could be similar to the shear mode of sand, where the particle rolling or transition would dominate during shear movement.

On the other hand, in sample B20 in faster shear rate stages as 1 mm/sec and 10 mm/sec, effective residual friction angles show approximately 13° which can be often measured in the tests using clay. Thus, the shear mode at faster shearing could be similar to the shear mode of clay, where the orientation of bentonite

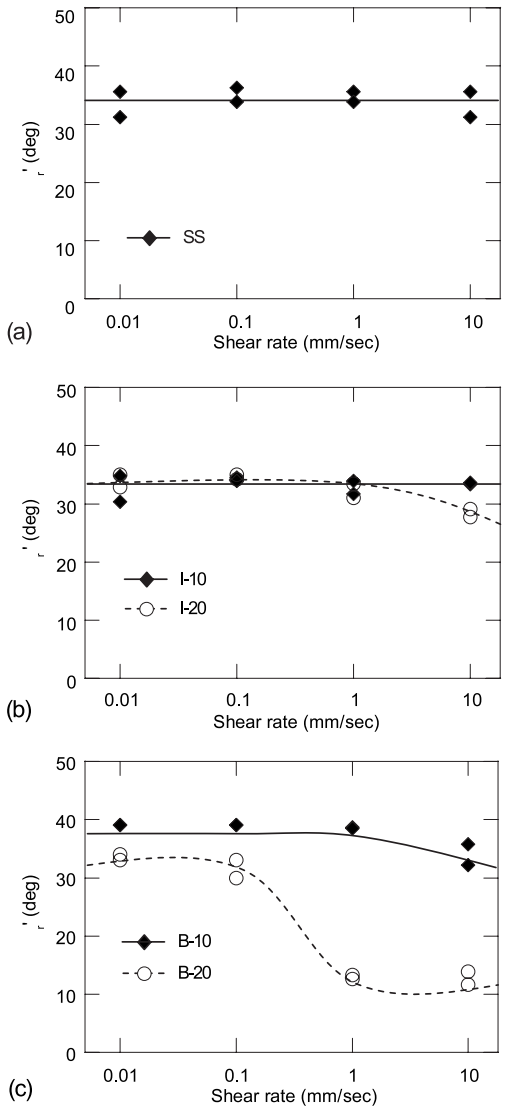

Fig. 9. Friction angle versus shear rate. (a) Silica sand No. 8. (b) Silica sand-Illite mixture sample. (c) Silica sand-Bentonite mixture sample.

would dominate during shear movement. Effective residual friction angles in silica sand-bentonite mixture samples could be combined values of their pure friction angles. The change in shear mode by shear rate would cause the rate effect mechanism of residual shear strength in cohesive soil.

Conclusions

The undrained ring shear tests were carried out with different shear rate in Silica sand, Silica sand-Illite mixture sample and Silica sand-Bentonite mixture sample, and the following conclusions could be drawn:

a) Residual friction angles were calculated by directly measured parameter: total normal stress, shear resistance and pore water pressure. As a result, the dependence of effective residual friction angle on shear rate was identified.

   Effective residual friction angle of silica sand was independent of shear rate, however, that of illite and bentonite mixture sample were dependent on shear rate.

b) According to the dependence of effective residual friction angle on shear rate, shear mode seems to change with shear rate. This change in shear mode could be thought as the rate effect mechanism of residual shear strength in cohesive soil.

Acknowledgements

The authors wish to thank Assistant Professor F. Wang and G. Wang of the Disaster Prevention Research Institute, Kyoto University, Japan, for their valuable support. We also wish to thank Technical Assistant Mr. K. Kondo, for maintenance and repair of the apparatus.

References

Lambe, T. W., Whitman, R. V. (1969):Soil Mechanics. Wiley Eastern Limited, New Delhi. 559p.

Lemos, J. L. J. (2003). Shear behavior of pre-existing shear zone under fast loading-insights on the landslide motion. *Proc. International workshop on occurrence and mechanisms of flow-like landslide motion*, p. 229–236.

Matsui, T., Ohara, H. and Ito, T. (1977). EFFECTS OF DYNAMIC STRESS HISTORY ON MECHANICAL CHARACTERISTICS SATURATED CLAYS. Journals of the Japan Society of Civil Engineers 257, p. 41–51. (in Japanese)

Sassa, K. Fukuoka, H. Wang, G. (2003). Performing undrained shear tests on saturated sands in a new intelligent type of ring-shear apparatus. *Geotechnical Testing Journal* 26, No. 3, p.257–265.

Sassa, K., Fukuoka, H., Wang, G., Ishikawa, H. (2004). Undrained dynamic-loading ring-shear apparatus and its application to landslide dynamics. *Landslide* 1, No. 1, p.9–17.

Skempton, A. W. (1985). Residual strength of clays in landslides, folded strata and the laboratory. *Géotechnique* 35, No. 1, p.3–18.

Suzuki, M., Umezaki, T., and Yamamoto, T. (2000). RESIDUAL STRENGTH OF SOIL BY DIRECT SHEAR TEST. *JOURNAL OF GEOTECHNICAL ENGINEERING* 645/III-50, JSCE, p.51–62.

Tika, T. E., Vaughan, P. R., Lemos, L. J. L. J. (1996). Fast shearing of pre-existing shear zone in soil. *Géotechnique* 46, No. 2, p.97–233.

Tika, T. E., Hutchinson, J. N. (1999). Ring shear tests on soil from the Vaiont landslide slip surface. *Géotechnique* 49, No. 1, p.59–74.